

MTL TR 92-34

AD-A254 905



2

# **SURFACE ANALYSIS OF $\text{Ln}_{2-x}\text{Ce}_x\text{CuO}_4$ (Ln = Pr AND Nd) SINGLE CRYSTALS GROWN BY THE TOP SEEDED SOLUTION METHOD**

**LOUISE C. SENGUPTA**

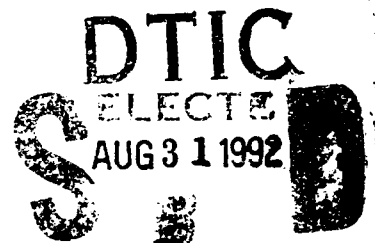
U.S. ARMY MATERIALS TECHNOLOGY LABORATORY  
CERAMICS RESEARCH BRANCH

**SOMNATH SENGUPTA**

MASSACHUSETTS INSTITUTE OF TECHNOLOGY  
CAMBRIDGE, MA

**WENDY E. KOSIK and J. DEREK DEMAREE**

U.S. ARMY MATERIALS TECHNOLOGY LABORATORY  
METALS RESEARCH BRANCH



May 1992

Approved for public release; distribution unlimited.



598580  
92-23962  
1994

U.S. ARMY MATERIALS TECHNOLOGY LABORATORY  
Watertown, Massachusetts 02172-0001

92 8 28 064

UNCLASSIFIED

**SECURITY CLASSIFICATION OF THIS PAGE (When Data Entered)**

UNCLASSIFIED

SECURITY CLASSIFICATION OF THIS PAGE (When Data Entered)

Block No. 20

**ABSTRACT**

Large single crystals of  $\text{Ln}_{2-x}\text{Ce}_x\text{CuO}_4$  ( $\text{Ln} = \text{Pr}$  and  $\text{Nd}$ ), the average size is approximately 5 mm x 5 mm x 1 mm, were grown by the Top Seeded Solution Growth (TSSG) technique. The optical constants of the crystals were determined by Variable Angle Spectroscopic Ellipsometry (VASE) and the results seem to indicate that a 1.5 eV absorption peak appears in the undoped material and is weakened and shifted downward in energy upon annealing. The compositions and crystal structure were examined using Rutherford Backscattering Spectroscopy (RBS) with ion beam channeling. Also, the effect of annealing on the crystalline structure was probed by ion beam channeling. The orientation and lattice parameters of the crystals were determined by X-ray diffraction and the superconductivity of the specimens was monitored using a SQUID magnetometer. The results indicate that the crystals grown by the TSSG method are very uniform in composition and well-oriented; however, analysis of the RBS data indicated up to 1% Pt inclusion in the crystals from contact with the Pt crucibles. The inclusion of Pt acted to quench the superconducting transition temperatures and Pt was found to substitute for Cu.

UNCLASSIFIED

SECURITY CLASSIFICATION OF THIS PAGE (When Data Entered)

## CONTENTS

	Page
INTRODUCTION .....	1
EXPERIMENTAL .....	1
RESULTS AND DISCUSSION .....	
RBS Results .....	2
VASE Results .....	7
CONCLUSIONS .....	11
ACKNOWLEDGMENTS .....	11
REFERENCES .....	11

DTIC QUALITY INSPECTED 3

Accession For	
NTIS GRA&I	<input checked="" type="checkbox"/>
DTIC TAB	<input type="checkbox"/>
Unannounced	<input type="checkbox"/>
Justification	<input type="checkbox"/>
By _____	
Distribution/ _____	
Availability Codes	
Dist	Avail and/or Special
A-1	

## INTRODUCTION

Since the discovery of the n-type superconductors<sup>1</sup> many workers have investigated the electron mediated superconduction mechanism<sup>2,3</sup> and attempted to produce single crystals using Top Seeded Solution Growth (TSSG),<sup>4</sup> Traveling Solvent Floating Zone (TSFZ),<sup>5</sup> and other methods such as the CuO flux method.<sup>6-9</sup> Also, several investigators have examined the optical properties of both the ceramic and single crystal forms of the n-type superconductor.<sup>8,10,11</sup>

In this study, the TSSG technique has been used to obtain single crystals of  $\text{Ln}_{2-x}\text{Ce}_x\text{CuO}_4$  ( $\text{Ln} = \text{Nd}$  and  $\text{Pr}$ ). This technique, unlike other growth procedures, can produce large specimens that contain fairly uniform dopant distributions.<sup>4</sup> A systematic study of the effect of Ce dopant and annealing on the optical spectra of the as-grown crystals was monitored using Variable Angle Ellipsometry Spectroscopic (VASE). The study also presents, for the first time (to our knowledge), a systematic examination of the effect of annealing and Ce-doping on the crystalline structure of the specimens as examined by ion beam channeling and Rutherford Backscattering Spectroscopy (RBS).

## EXPERIMENTAL

The TSSG method had been described by Belruss, et al.<sup>12</sup> in a previous article. The growth of pure and Ce doped  $\text{Nd}_2\text{CuO}_4$  using TSSG has been discussed by Cassanho, et al.<sup>4</sup> The  $\text{Pr}_2\text{CuO}_4$  single crystals (doped and undoped) were also grown in a similar fashion by A. Cassanho.  $\text{Ln}_{2-x}\text{Ce}_x\text{CuO}_4$  ( $\text{Ln} = \text{Nd}$  and  $\text{Pr}$ ) has a tetragonal crystal structure. The specimens used in this experiment were c-axis oriented which indicates that the c-axis is perpendicular to the crystal surface. The as-grown samples were analyzed using the techniques mentioned above. The details of the RBS and VASE apparatus for each experiment will be described below. The crystals were subsequently annealed at  $950^\circ\text{C}$  for about 15 hours under flowing argon. The samples were then re-examined.

The RBS technique involves the acceleration of  $\text{He}^+$  ions to 2 MeV by a National Electrostatics Corporation (NEC) tandem pelletron accelerator. This  $\text{He}^+$  ion beam is collimated to a 1 mm diameter beam which is incident upon the crystal. The scattered helium ions were detected at a backscattering angle of  $170^\circ$  with a surface barrier detector. The energy resolution of the detection system is 20 KeV to 25 KeV. The (001) channeled spectra were obtained by rotating the samples about the beam axis ( $\phi$ ), and perpendicular to it ( $\theta$ ), until a minimum yield was located. The minima in the backscattering yield occurs when the incident beam is aligned with the planar and/or axial directions in the crystal; i.e., channeling. When the beam is not aligned in either the axial or planar directions of the crystal, no channeling is present and the *random* spectrum is obtained. The energy detection system is calibrated with a standard prior to data acquisition. The elements in the crystal are identified from the mass of the atoms which are determined from the detected energies of the backscattered ions. The composition of the specimens were obtained by utilizing the software program RUMP to fit a simulation to the data.<sup>13</sup>

The ellipsometry data was obtained using a J. A. Woollam VASE. In this system, the elliptically-polarized light produced by reflecting plan-polarized light from the surface under study is modulated by a rotating analyzer. Both the wavelength of the monochromatic incident light and the angle of incidence can be varied. At each wavelength after 150 revolutions of the analyzer, a data acquisition program subtracts a reading obtained

with the shutter closed from a reading obtained with the shutter open. During a measurement, the wavelength scanned from 4000 Å to 8000 Å at steps of 100 Å. Two or three angles of incidence were examined at each spot.

## RESULTS AND DISCUSSION

### RBS Results

Figures 1a, 1b, 2a, and 2b show the random and channeled RBS spectra of  $\text{Nd}_2\text{CuO}_4$  and  $\text{Nd}_{2-x}\text{Ce}_x\text{CuO}_4$  single crystals. Figures 1b and 2b show an expanded energy scale (x-axis) of the channeled spectra. Similar spectra for  $\text{Pr}_2\text{CuO}_4$  and  $\text{Pr}_{2-x}\text{Ce}_x\text{CuO}_4$  single crystals are shown in Figures 3a, 3b, 4a, and 4b, respectively. Again, Figures 3b and 4b display an expanded energy scale (x-axis). The horizontal axis is proportional to the energy at which the backscattered ion was detected. The vertical axis is the normalized yield. The ratio of the elements (in atomic %) were determined by the best fit of the RUMP simulation. The composition in Figure 2 could not be accurately analyzed since the *random* spectrum was not entirely random, creating difficulty in obtaining a good fit of the simulation to the experimental data. For Figures 1, 3, and 4 the ratio of the elements and the minimum yield obtained for each element (from the channeled spectra) are given in Table 1.

Table 1. ELEMENTAL PROPORTIONS (ATOMIC %) AND MINIMUM YIELDS (%) OBTAINED FROM THE BEST RUMP FIT TO THE RBS DATA FOR  $\text{Ln}_{2-x}\text{Ce}_x\text{O}_4$  ( $\text{Ln} = \text{Nd}$  AND  $\text{Pr}$ )

Sample	Pr (%), Min. Yield (%)	Nd (%), Min. Yield (%)	Ce (%), Min. Yield (%)	Cu (%), Min. Yield (%)	O (%), Min. Yield (%)	Pt (%), Min. Yield (%)
$\text{Nd}_2\text{CuO}_4$	---	26.0, 5	---	15.1, 10	58.0, ---	0.9, 40
$\text{Nd}_{2-x}\text{Ce}_x\text{CuO}_4$	---	---	---	---	---	---
$\text{Pr}_2\text{CuO}_4$	29.0, 5	---	---	12.0, 5	58.0, ---	1.0, 5
$\text{Pr}_{2-x}\text{Ce}_x\text{CuO}_4$	22.1, 4	---	4.5, 4	14.4, 40	58.4, ---	0.6, 40

As shown in Figures 2 and 4, Nd/Ce and Pr/Ce cannot be distinguished on the RBS spectra due to similar mass (energy), so in the simulation  $x = 0.17$  Ce is used in place of Pr in the doped specimens, which was found from the lattice parameter,  $c$  (Å), obtained from the X-ray powder diffraction data and given in Table 2. The value for  $c$  (Å) has been shown to be directly related to the Ce content in the material,<sup>6</sup> and the values extrapolated from this relationship for Ce ( $x$ ) are also given in Table 2.

Table 2. LATTICE PARAMETERS AND CORRESPONDING Ce ( $x$ )  
(FROM REFERENCE 6) OF  $\text{Ln}_{2-x}\text{Ce}_x\text{CuO}_4$  ( $\text{Ln} = \text{Nd}$  AND  $\text{Pr}$ )  
OBTAINED FROM THE X-RAY DIFFRACTION DATA

Sample	$c$ (Å)	Ce ( $x$ )
$\text{Nd}_2\text{CuO}_4$	12.17	0
$\text{Nd}_{2-x}\text{Ce}_x\text{CuO}_4$	12.07	0.17
$\text{Pr}_2\text{CuO}_4$	12.26	0
$\text{Pr}_{2-x}\text{Ce}_x\text{CuO}_4$	12.16	0.15

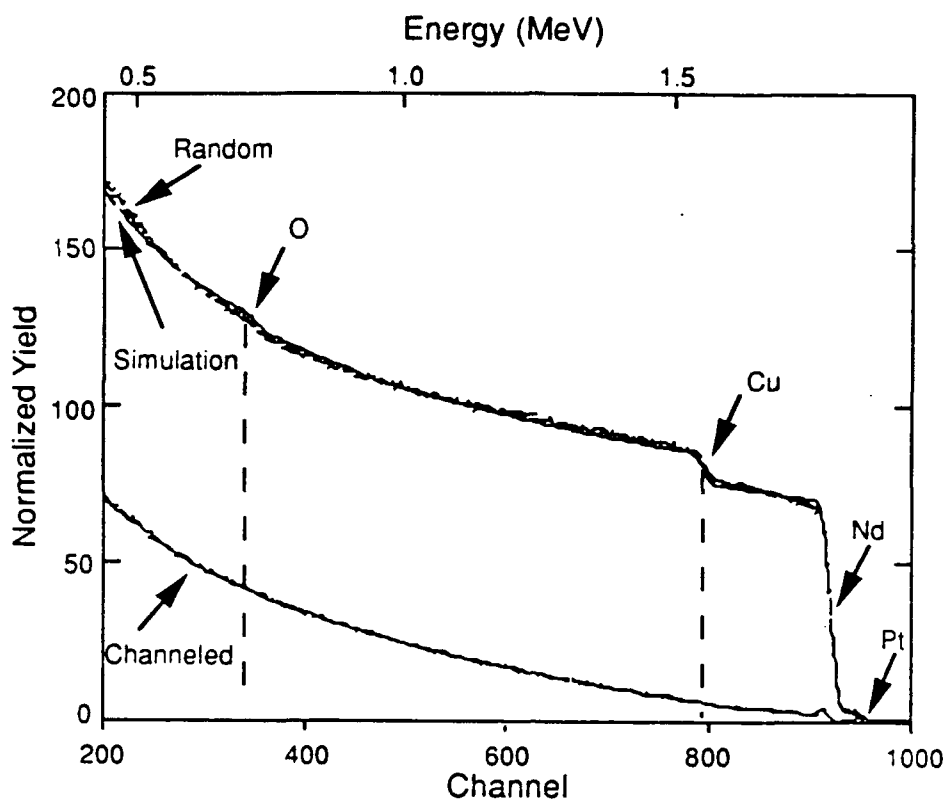


Figure 1(a). Random and channelled RBS spectra and simulation obtained from a fit to data for  $\text{Nd}_2\text{CuO}_4$ .

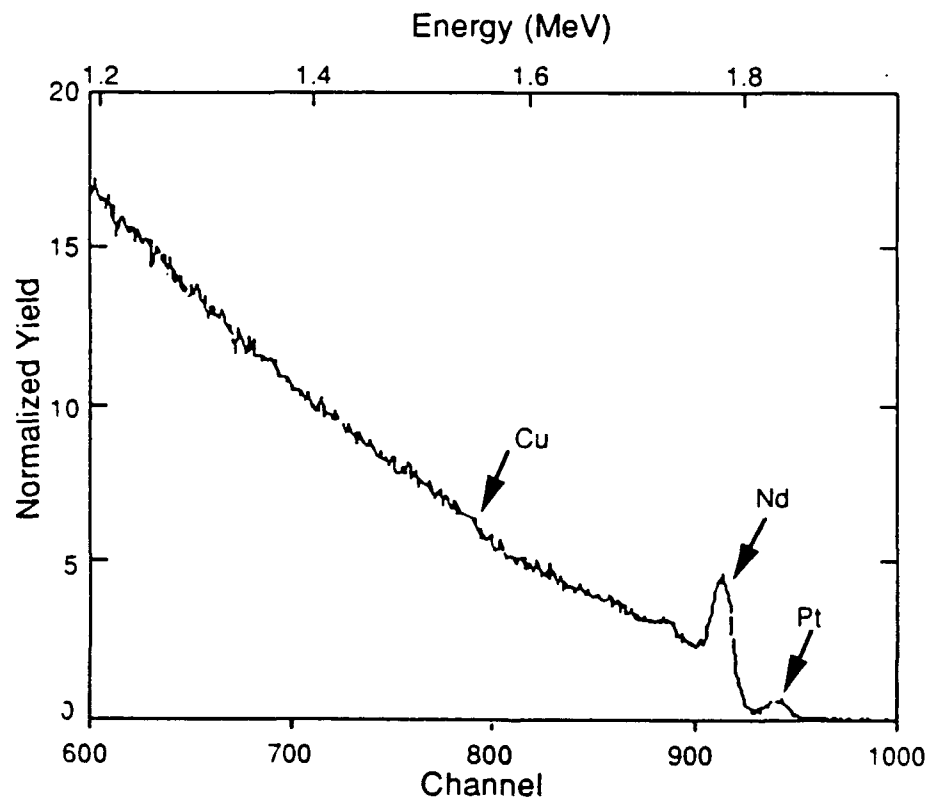


Figure 1(b). Expanded energy scale (x-axis) for the channelled spectra shown in Figure 1(a).

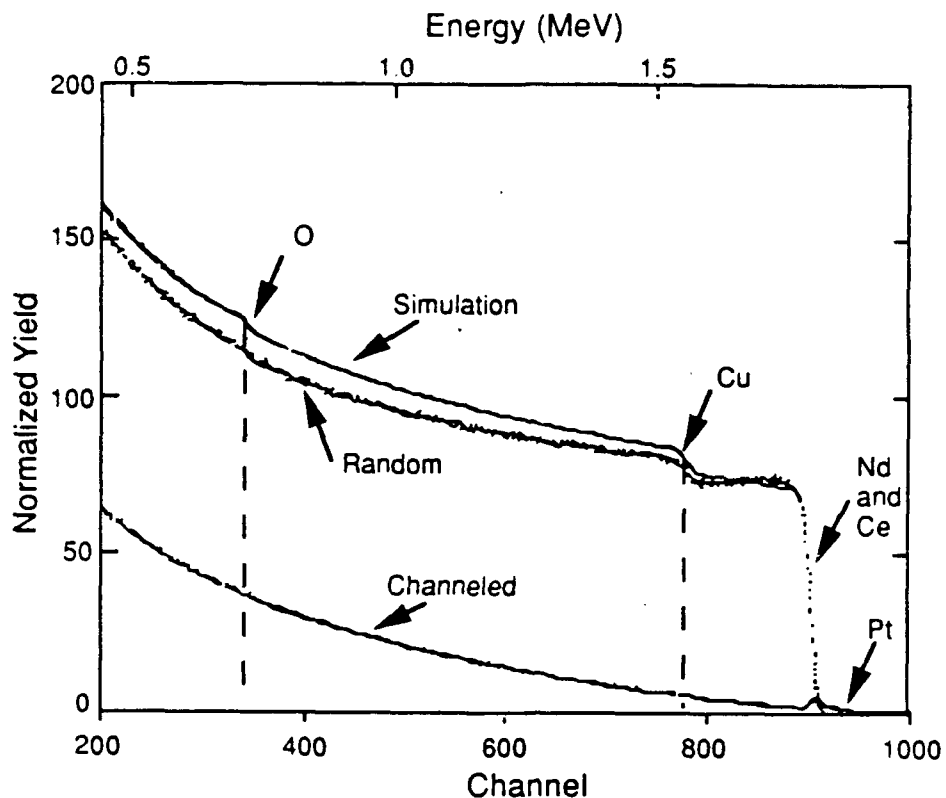


Figure 2(a). Random and channeled RBS spectra obtained from a fit to data for  $\text{Nd}_{2-x}\text{Ce}_x\text{CuO}_4$ .

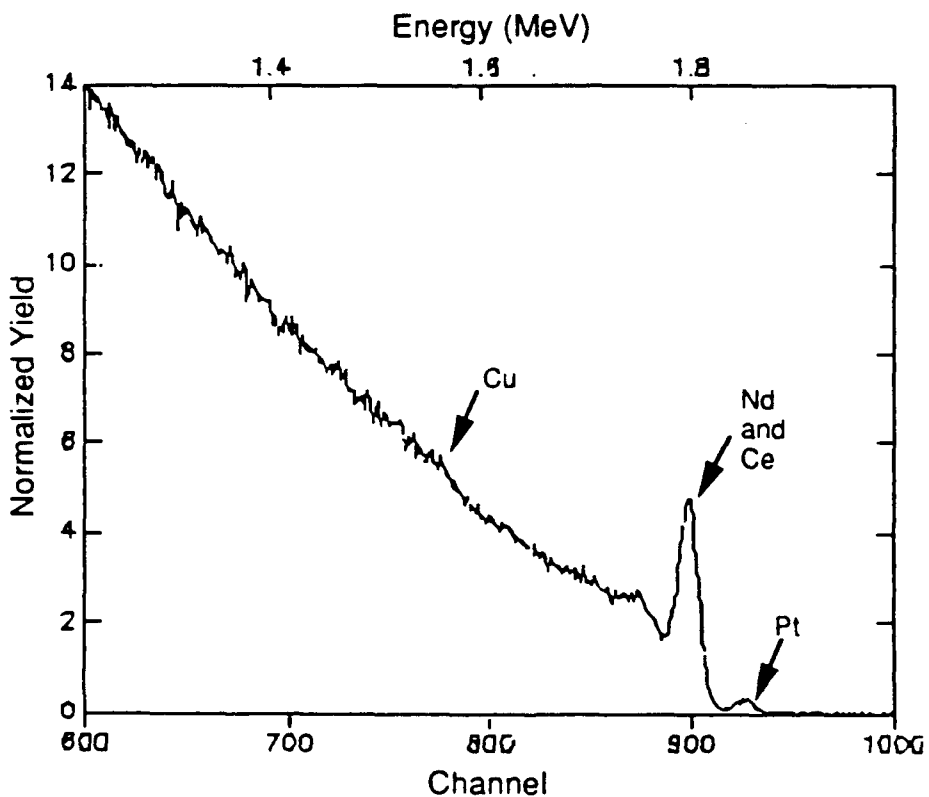


Figure 2(b). Expanded energy scale (x-axis) for the channeled spectra shown in Figure 2(a).

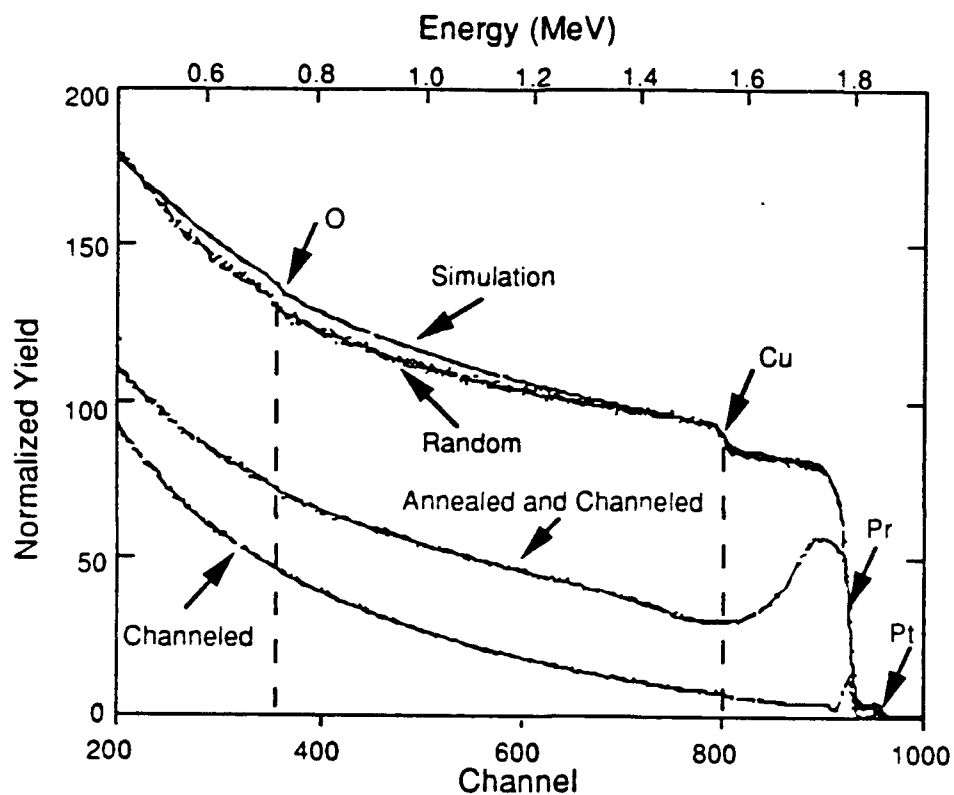


Figure 3(a). Random and channelled RBS spectra and simulation obtained from a fit to data for  $\text{Pr}_2\text{CuO}_4$ .

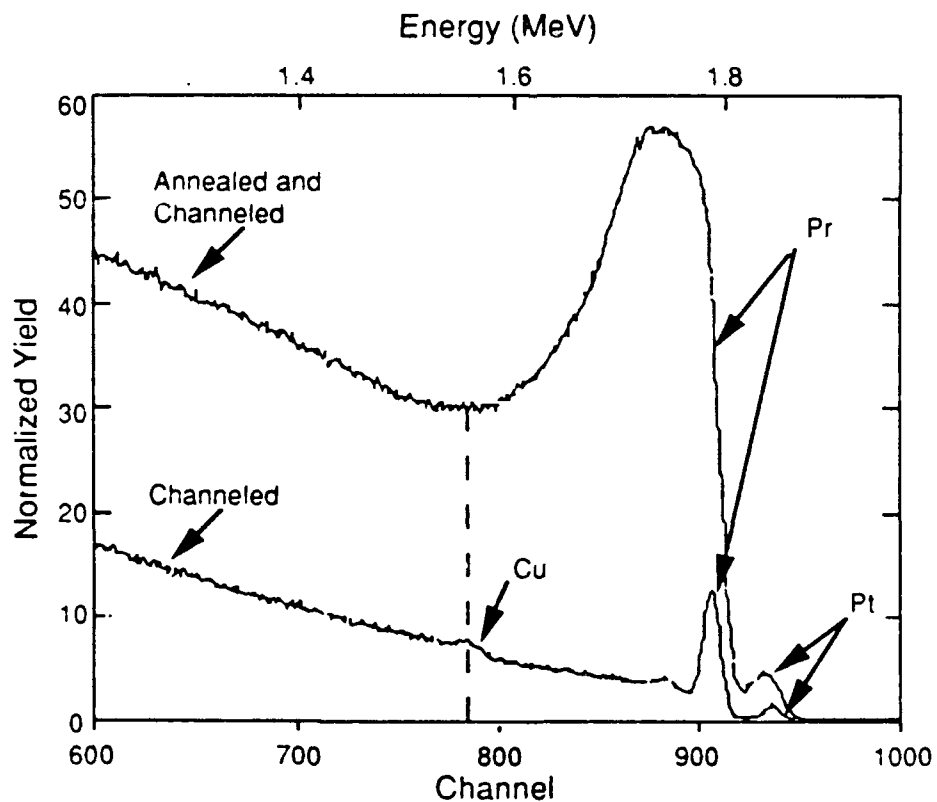


Figure 3(b). Expanded energy scale (x-axis) for the channelled spectra shown in Figure 3(a).

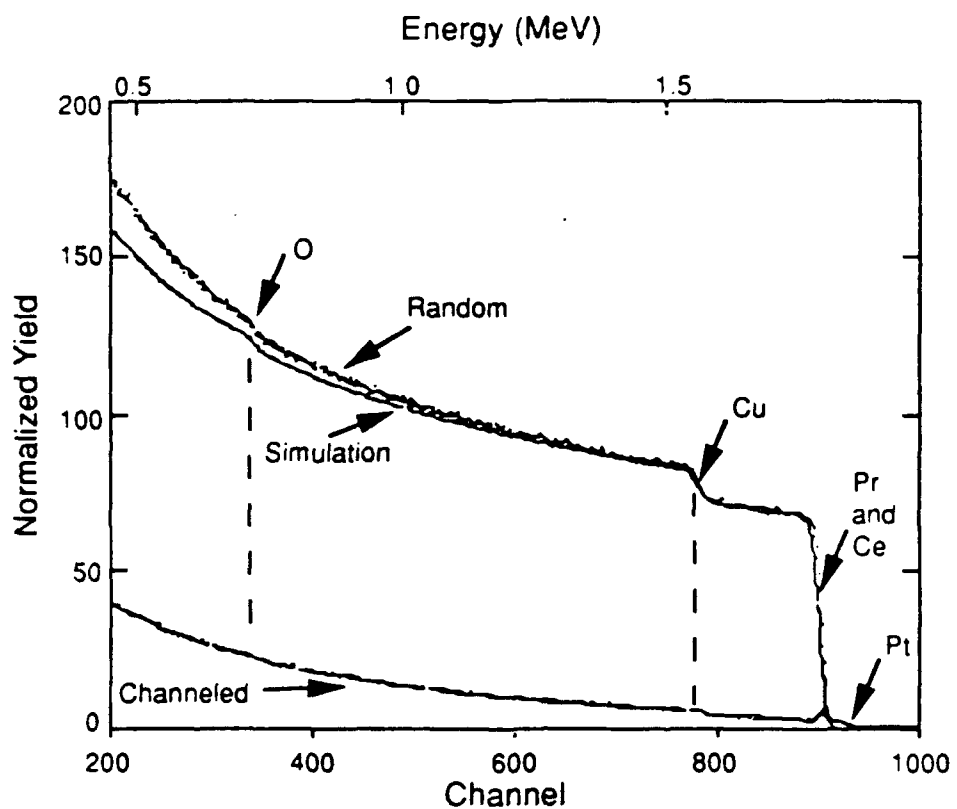


Figure 4(a). Random and channelled RBS spectra and simulation obtained from a fit to data for  $\text{Pr}_{2-x}\text{Ce}_x\text{CuO}_4$ .

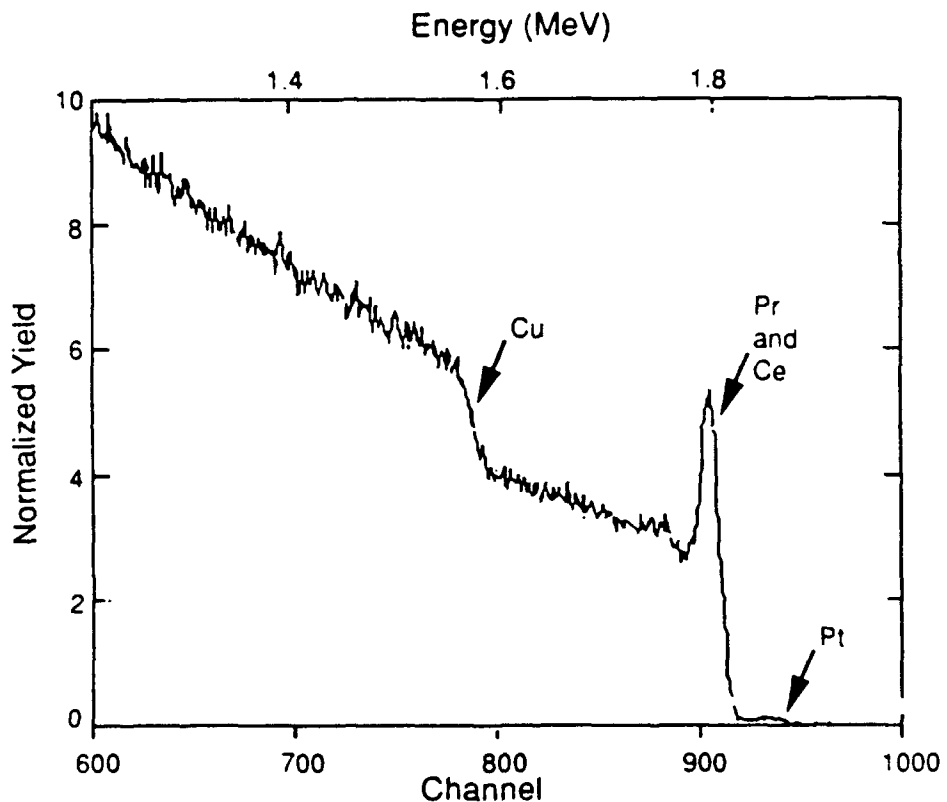


Figure 4(b). Expanded energy scale (x-axis) for the channelled spectra shown in Figure 4(a).

As seen in the Figures, Pt (up to 1%) is incorporated into the crystal through contamination by the crucible. It should be noted that the Pt is seen to channel and can be observed by the definite appearance of sharp surface peak and a low minimum yield in the channeled spectra. This indicates that Pt is substitutional throughout the crystal. It is assumed Pt substitutes for Cu in the specimen, as was seen in a previous report,<sup>9</sup> and is not merely on the sample surface. This substitution causes the critical temperature,  $T_c$ , to decrease to a value outside of our range of measurement with the SQUID magnetometer ( $\sim 4K$ ).

A small peak is located immediately to the left of Nd/Pr/Ce, as shown in Figures 1 through 4. This peak may be due to an impurity such as Ag, In, Sn, Sb, or Cd. The impurity may contribute to the roll-off of the front edge of the *random* spectrum obtained for the  $Pr_{2-x}Ce_xCuO_4$  sample seen in Figure 4.

In general, the minimum yield obtained for the elements, as seen in Table 1, is very low indicating that the sample is well-oriented and the crystalline structure is very well-ordered. Channeling occurs when the He ion is steered by the electrostatic repulsion of the nuclei located at the lattice sites and the probability that He will be backscattered is decreased except at the surface (as indicated by the surface peak). The yield attenuations occur for atoms in the lattice structure and/or any atoms in a substitutional site or shadowed by the lattice structure for that planar orientation. However, any atoms not in the lattice structure will be hit with the ion beam and are, therefore, identified as being an interstitial atom. As shown in the figures, none of the elements appear to contain interstitial species since channeling occurs for all of the elements in all of the specimens. However, as shown in Figure 4, for the  $Pr_{2-x}Ce_xCuO_4$  sample, Cu/Pt do not channel as well, as indicated by the higher yield and the fact that the Cu/Pt do not appear as peaks but as ledges. Since both Pt and Cu seem to channel poorly in this specimen, it confirms the fact that Pt does indeed substitute for Cu in the material. Also, the poor channeling may indicate that Cu/Pt are slightly displaced from the lattice sites. Previous workers have noticed a bending of the Cu-O chains upon doping the materials.<sup>6</sup> The Ce doping may cause the distortion in Cu/Pt sites, especially since this was not observed for the  $Pr_2CuO_4$  sample.

Finally, the channeled spectrum for the annealed  $Pr_2CuO_4$  sample is shown in Figure 3. As shown in the figure, the minimum yield obtained for Pr in the specimen has increased to  $\sim 30\%$ . However, the yield is not as high as in the random spectrum; this implies some disorder, from the creation of oxygen vacancies and/or surface realignment, but not a totally disordered material. Also, the back ledge of the spectrum does not have as low a yield as the unannealed specimens but it is reduced from the random spectra. This could be due to the disorder caused by the presence of oxygen vacancies throughout the crystal or by dechanneling of the helium ions after scattering through a disordered surface. Further studies in which the surfaces of the specimens will be etched and re-examined will be carried out in the future.

#### VASE Results

In Figures 5 and 6, the VASE spectra of the imaginary part of the dielectric function  $\epsilon_2$  for undoped  $Nd_2CuO_4$  and  $Pr_2CuO_4$  are shown. As shown in the figures, an absorption peak at 1.5 eV ( $\sim 8000 \text{ \AA}$ ) is observed. This absorption peak has been assigned to a bound charge transfer (CT) excitation from the Cu(3d) to O(2p) in the Cu oxygen plane.<sup>8,10,11</sup> The transition has been observed for p-type superconductors at 1.7 eV for  $YBa_2Cu_3O_{7-\delta}$ <sup>10</sup> and at 2 eV for  $LaCuO_4$ .<sup>10</sup> The transition is more pronounced in these n-type superconductors even though the coordination in the  $CuO_2$  planes is fourfold rather than fivefold or sixfold as in

the case of the p-type superconductors. This may be due to the fact that the c/a ratio of the lattice parameters is significantly smaller in the n-type material which indicates an increase in the ionicity of the bonds. The sharpness of the transition may also be due to the lack of a decay channel for the excited carrier.<sup>8</sup> In Figure 7, the VASE spectrum of  $\epsilon_2$  of the annealed  $\text{Pr}_2\text{CuO}_4$  sample is shown (inset shows spectrum with an expanded scale, y-axis). As the material is annealed, the oscillator strength for the transition is decreased (transition is weakened) and it is slightly shifted downward in energy. The weakening and downward shift of the absorption peak may be caused by the opening of a decay channel for the charge carrier. This decay channel may be viewed as disorder in the material caused by the presence of oxygen vacancies as indicated by the RBS data.

In Figures 8 and 9 (inset shows an expanded scale for the y-axis), VASE spectra of  $\epsilon_2$  for  $\text{Nd}_{2-x}\text{Ce}_x\text{CuO}_4$  and  $\text{Pr}_{2-x}\text{Ce}_x\text{CuO}_4$  are shown. The spectra indicate that as the material becomes conducting upon doping with Ce, the 1.5 eV transition is no longer observed. Again, this is similar to the case with the p-type superconductors; e.g., Sr doping in  $\text{La}_{2-x}\text{Sr}_x\text{CuO}_4$ .<sup>10</sup> As shown in the RBS data the suppression of the transition is not from the creation of a disordered material; i.e., the creation of oxygen vacancies, but rather from the introduction of free-carriers which act to produce screening of the  $\text{CuO}_2$  planes. Since similar behavior occurs for p-type and n-type superconductors, it seems apparent that either type carrier may serve to suppress this transition.

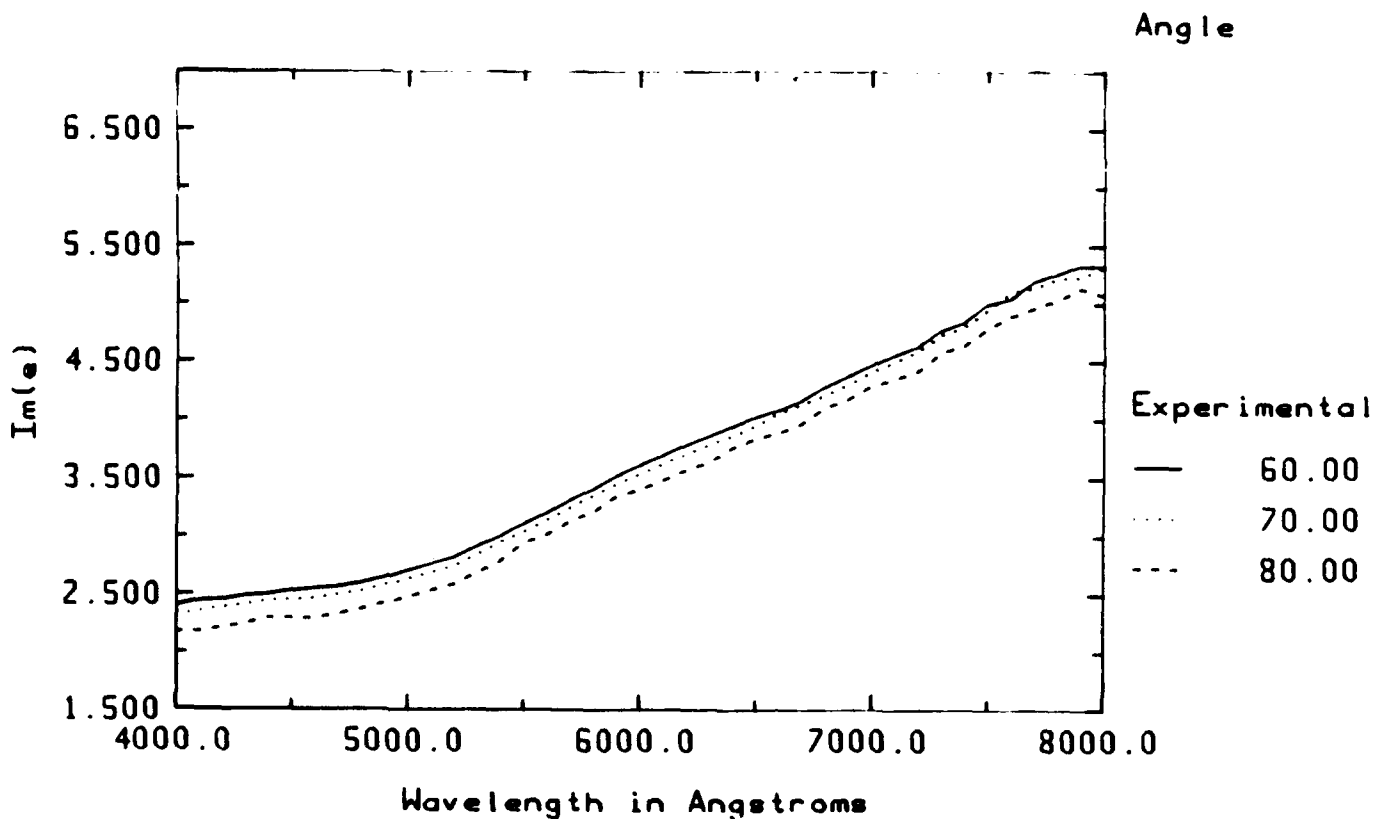


Figure 5. VASE spectrum of the imaginary part of the dielectric function,  $\epsilon_2$ , versus wavelength for  $\text{Nd}_2\text{CuO}_4$ ,  $\theta_i = 60^\circ, 70^\circ$ , and  $80^\circ$ .

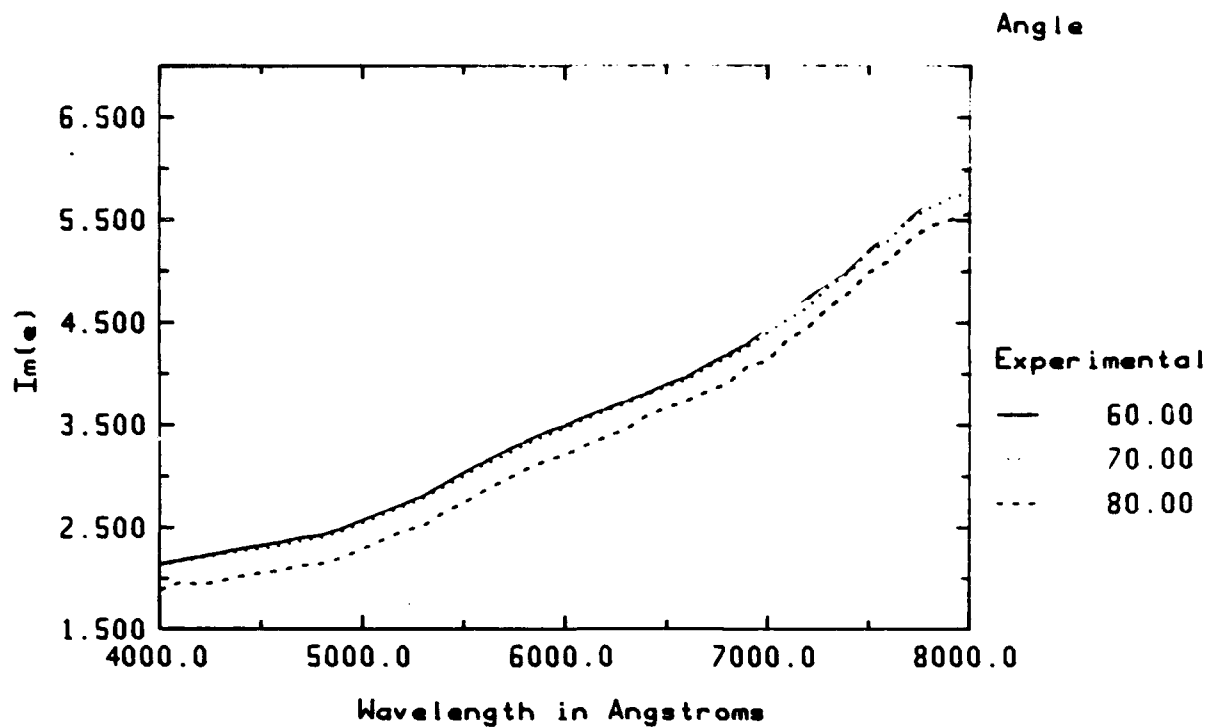


Figure 6. VASE spectrum of the imaginary part of the dielectric function,  $\epsilon_2$ , versus wavelength for  $\text{Pr}_2\text{CuO}_4$ ,  $\theta_i = 60^\circ$ ,  $70^\circ$ , and  $80^\circ$ .

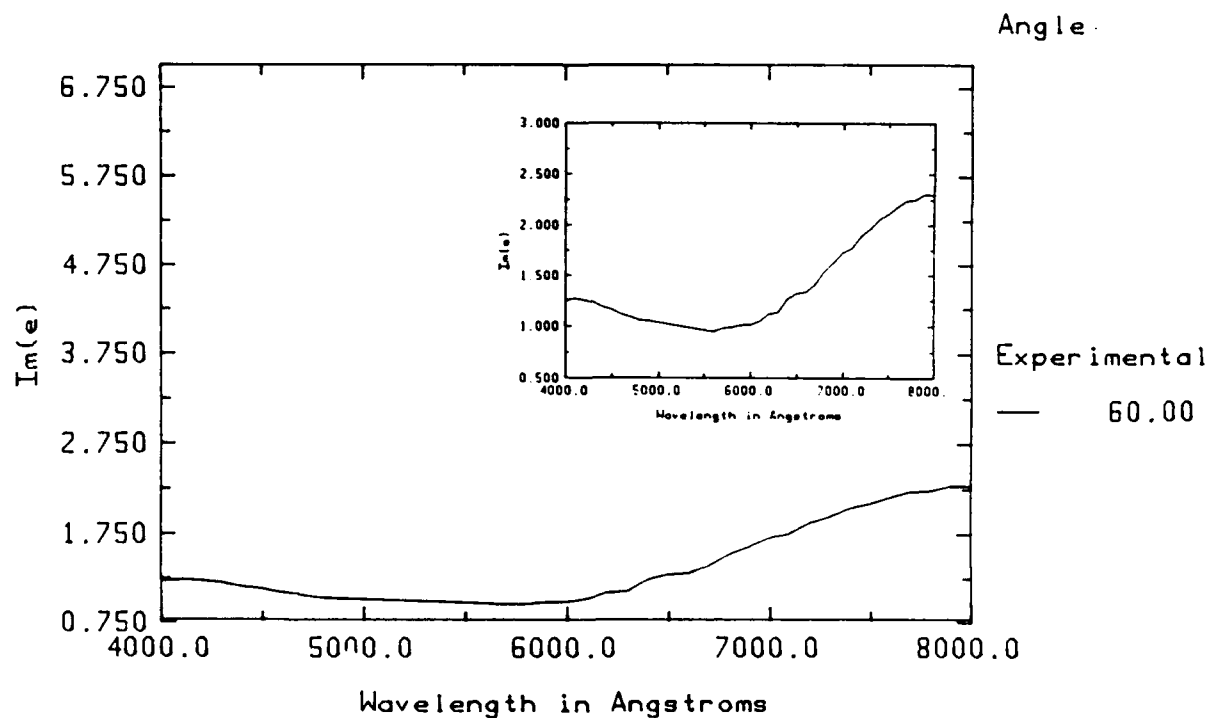


Figure 7. VASE spectrum of the imaginary part of the dielectric function,  $\epsilon_2$ , versus wavelength for the annealed  $\text{Pr}_2\text{CuO}_4$  specimen, (inset shows an expanded y-scale of the spectrum),  $\theta_i = 60^\circ$ .

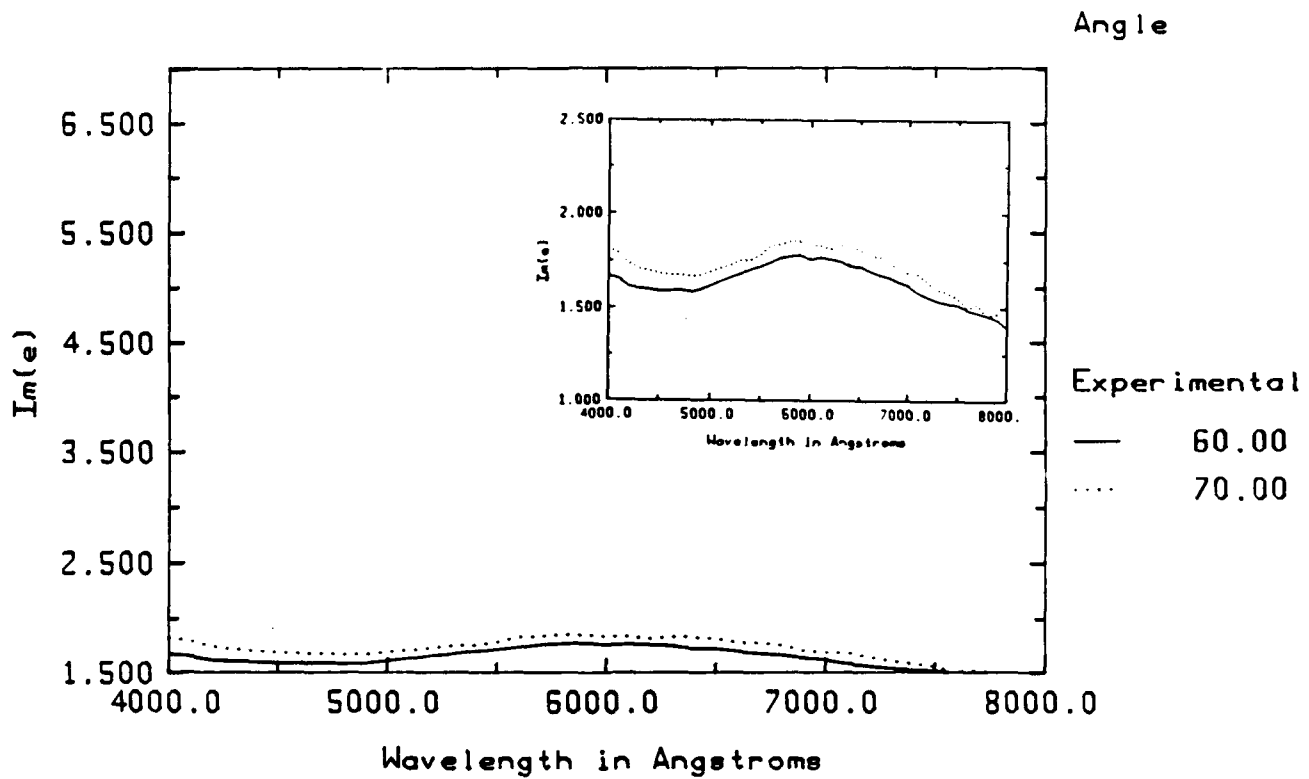


Figure 8. VASE spectrum of the imaginary part of the dielectric function,  $\epsilon_2$ , versus wavelength for the annealed  $\text{Nd}_{2-x}\text{Ce}_x\text{O}_4$  specimen, (inset shows an expanded y-scale of the spectrum),  $\theta_i = 60^\circ$  and  $70^\circ$ .

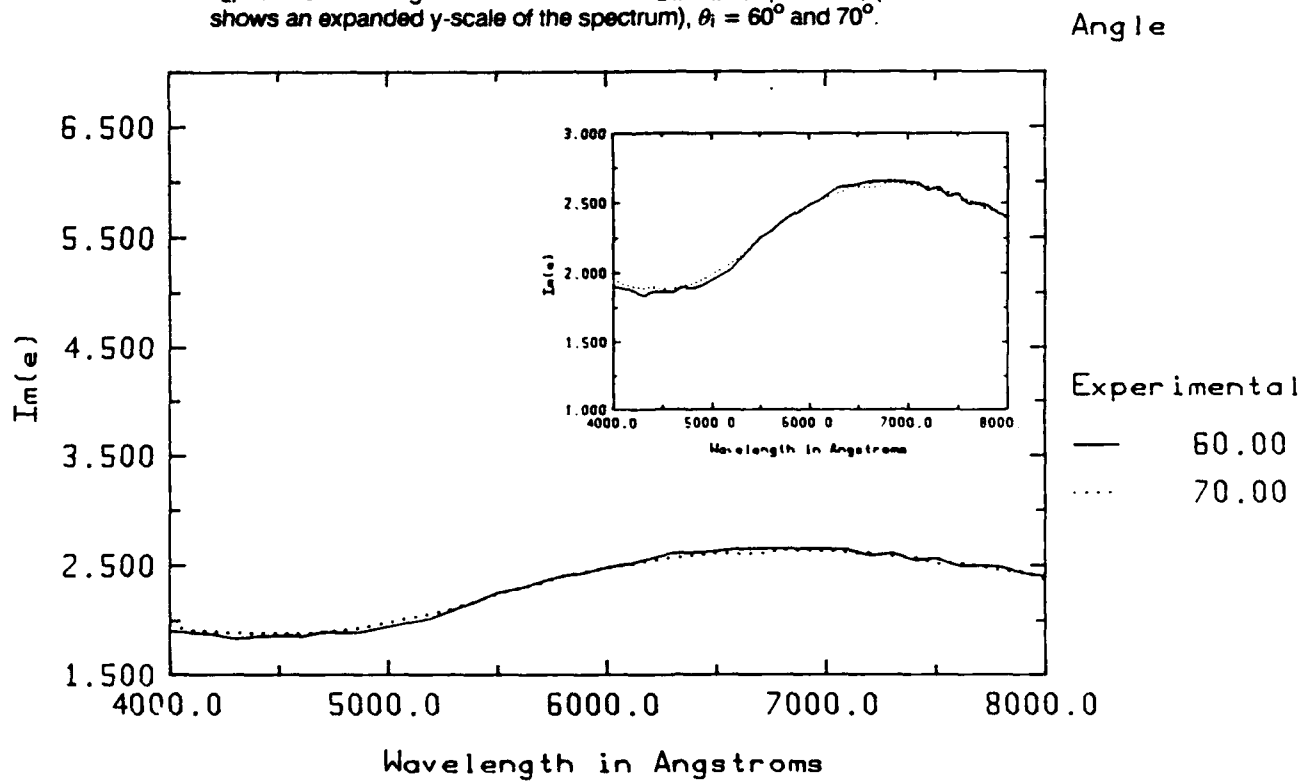


Figure 9. VASE spectrum of the imaginary part of the dielectric function,  $\epsilon_2$ , versus wavelength for  $\text{Nd}_{2-x}\text{Ce}_x\text{CuO}_4$  (inset shows an expanded y-scale of the spectrum),  $\theta_i = 60^\circ$  and  $70^\circ$ .

## CONCLUSIONS

The crystal structure and composition of the  $\text{Ln}_{2-x}\text{Ce}_x\text{CuO}_4$  ( $\text{Ln} = \text{Pr}$  and  $\text{Nd}$ ) samples were examined using RBS with ion channeling. The minimum yields obtained for the elements in the crystals indicate that the crystals are well-oriented and very ordered. The addition of Ce to the material causes a slight displacement of the Cu sites. Also, an additional inclusion of Pt (up to 1%) was found in the crystals. The Pt is incorporated into the material by contamination by the crucible and this amount was enough to quench the superconductivity. The annealed spectrum of the  $\text{Pr}_2\text{CuO}_4$  sample displays disorder which is either incorporated throughout the material or confined to a surface layer (which will be investigated by etching the crystal and re-examining).

The electronic structure of the n-type superconductors was investigated using VASE. An absorption peak is shown in the spectra of the imaginary part of the dielectric function,  $\epsilon_2$ , for the undoped samples which is assigned to a bound charge transfer transition from  $\text{Cu}(3d)$  to  $\text{O}(2p)$  in the  $\text{CuO}_2$  planes. The peak is weakened upon annealing due to the creation of decay channel for the carrier, and the absorption peak is quenched upon the addition of Ce in the material. The suppression of the peak by n-type carriers is thought to be due to an increase in the screening of the  $\text{CuO}_2$  planes. Further studies on the effect annealing on the electronic and crystalline structure of the samples will be carried out in the future.

## ACKNOWLEDGMENTS

Sommath Sengupta would like to acknowledge the support of MRL-N.S.F., Grant No. DMR-90-22933, and A. Cassanho for supplying the  $\text{Ln}_{2-x}\text{Ce}_x\text{CuO}_4$  ( $\text{Ln} = \text{Pr}$  and  $\text{Nd}$ ) crystals used in this study.

## REFERENCES

1. TOKURA, Y., TAKAGI, H., and UCHIDA, S. *Nature* 339, 1989, p. 345.
2. FORTUNE, N. A., MURATA, K., ISHIBASHI, M., YOKOYAMA, Y., and NISHIHARA, Y. *Physica B* 1969, 1991, p. 635.
3. UJI, S., OAKI, H., MATSUMOTO, T. *Japan. J. App. Phys.* 28, 1989, p. L563.
4. CASSANHO, A., GABBE, D. R., and JENSSSEN, H. P. *J. Crystal Growth* 96, 1988, p. 999.
5. KOJIMA, H., WATANBE, T., KOMAI, N., and TANAKA, I. *Mol. Cryst. Liq. Cryst.* 184, 1990, p. 69.
6. TARASCON, J. M., et al. *Phys. Rev. B* 40, 1989, p. 4494.
7. SAINT-PAUL, M., et al. *Solid State Commun.* 76, 1990, p. 1257.
8. TAJIMA, S., et al. *J. Opt. Soc. Am. B* 6, 1989, p. 475.
9. HIDAKA, Y. *Proc. of 2nd ISS '89*. T. Ishiguro and K. Kajimura, eds., Springer-Verlag, 1990, p. 229.
10. KELLY, M. K., BARBOUX, P., TARASCON, J. M., and ASPNES, D. E. *Phys. Rev. B* 40, 1989, p. 6797.
11. UCIDA, S., TAKAGI, H., and TOKURA, Y. *J. Less-Common-Metals* 164 and 165, 1990, p. 741.
12. BELRUSS, V., KALNAJS, J., LINZ, A., and FOLWEILLER, R. C. *Mater. Res. Bull.* 6, 1971, p. 899.
13. DOOLITTLE, L. R. *Nuclear Instr. Meth. B* 9, 1985, p. 334.

DISTRIBUTION LIST

No. of Copies	To
1	Office of the Under Secretary of Defense for Research and Engineering, The Pentagon, Washington, DC 20301
	Commander, U.S. Army Laboratory Command, 2800 Powder Mill Road, Adelphi, MD 20783-1145
1	ATTN: AMSLC-IM-TL
1	AMSLC-CT
	Commander, Defense Technical Information Center, Cameron Station, Building 5, 5010 Duke Street, Alexandria, VA 22304-6145
2	ATTN: DTIC-FDAC
1	MIA/CINDAS, Purdue University, 2595 Yeager Road, West Lafayette, IN 47905
	Commander, Army Research Office, P.O. Box 12211, Research Triangle Park, NC 27709-2211
1	ATTN: Information Processing Office
	Commander, U.S. Army Materiel Command, 5001 Eisenhower Avenue, Alexandria, VA 22333
1	ATTN: AMCSCL
	Commander, U.S. Army Materiel Systems Analysis Activity, Aberdeen Proving Ground, MD 21005
1	ATTN: AMXSY-MP, H. Cohen
	Commander, U.S. Army Missile Command, Redstone Scientific Information Center, Redstone Arsenal, AL 35898-5241
1	ATTN: AMSMI-RD-CS-R/Doc
1	AMSMI-RLM
	Commander, U.S. Army Armament, Munitions and Chemical Command, Dover, NJ 07801
2	ATTN: Technical Library
	Commander, U.S. Army Natick Research, Development and Engineering Center, Natick, MA 01760-5010
1	ATTN: Technical Library
	Commander, U.S. Army Satellite Communications Agency, Fort Monmouth, NJ 07703
1	ATTN: Technical Document Center
	Commander, U.S. Army Tank-Automotive Command, Warren, MI 48397-5000
1	ATTN: AMSTA-ZSK
1	AMSTA-TSL, Technical Library
	Commander, White Sands Missile Range, NM 88002
1	ATTN: STEWS-WS-VT
	President, Airborne, Electronics and Special Warfare Board, Fort Bragg, NC 28307
1	ATTN: Library
	Director, U.S. Army Ballistic Research Laboratory, Aberdeen Proving Ground, MD 21005
1	ATTN: SLCBR-TSB-S (STINFO)
	Commander, Dugway Proving Ground, UT 84022
1	ATTN: Technical Library, Technical Information Division
	Commander, Harry Diamond Laboratories, 2800 Powder Mill Road, Adelphi, MD 20783
1	ATTN: Technical Information Office
	Director, Benet Weapons Laboratory, LCWSL, USA AMCCOM, Watervliet, NY 12189
1	ATTN: AMSMC-LCB-TL
1	AMSMC-LCB-R
1	AMSMC-LCB-RM
1	AMSMC-LCB-RP
	Commander, U.S. Army Foreign Science and Technology Center, 220 7th Street, N.E., Charlottesville, VA 22901-5396
3	ATTN: AIFRTC, Applied Technologies Branch, Gerald Schlesinger
	Commander, U.S. Army Aeromedical Research Unit, P.O. Box 577, Fort Rucker, AL 36360
1	ATTN: Technical Library

No. of Copies	To
	Commander, U.S. Army Aviation Systems Command, Aviation Research and Technology Activity, Aviation Applied Technology Directorate, Fort Eustis, VA 23604-5577
1	ATTN: SAVDL-E-MOS
	U.S. Army Aviation Training Library, Fort Rucker, AL 36360
1	ATTN: Building 5906-5907
	Commander, U.S. Army Agency for Aviation Safety, Fort Rucker, AL 36362
1	ATTN: Technical Library
	Commander, USACDC Air Defense Agency, Fort Bliss, TX 79916
1	ATTN: Technical Library
	Commander, Clarke Engineer School Library, 3202 Nebraska Ave., N, Ft. Leonard Wood, MO 65473-5000
1	ATTN: Library
	Commander, U.S. Army Engineer Waterways Experiment Station, P.O. Box 631, Vicksburg, MS 39180
1	ATTN: Research Center Library
	Commandant, U.S. Army Quartermaster School, Fort Lee, VA 23801
1	ATTN: Quartermaster School Library
	Naval Research Laboratory, Washington, DC 20375
1	ATTN: Code 5830
2	Dr. G. R. Yoder - Code 6384
	Chief of Naval Research, Arlington, VA 22217
1	ATTN: Code 471
1	Edward J. Morrissey, WRDC/MLTE, Wright-Patterson Air Force Base, OH 45433-6523
	Commander, U.S. Air Force Wright Research & Development Center, Wright-Patterson Air Force Base, OH 45433-6523
1	ATTN: WRDC/MLLP, M. Forney, Jr.
1	WRDC/MLBC, Mr. Stanley Schulman
	NASA - Marshall Space Flight Center, MSFC, AL 35812
1	ATTN: Mr. Paul Schuerer/EH01
	U.S. Department of Commerce, National Institute of Standards and Technology, Gaithersburg, MD 20899
1	ATTN: Stephen M. Hsu, Chief, Ceramics Division, Institute for Materials Science and Engineering
1	Committee on Marine Structures, Marine Board, National Research Council, 2101 Constitution Avenue, N.W., Washington, DC 20418
1	Librarian, Materials Sciences Corporation, 930 Harvest Drive, Suite 300, Blue Bell, PA 19422
1	Charles Stark Draper Laboratory, 68 Albany Street, Cambridge, MA 02139
	Wyman-Gordon Company, Worcester, MA 01601
1	ATTN: Technical Library
	General Dynamics, Convair Aerospace Division P.O. Box 748, Fort Worth, TX 76101
1	ATTN: Mfg. Engineering Technical Library
	Plastics Technical Evaluation Center, PLASTEC, ARDEC Bldg. 355N, Picatinny Arsenal, NJ 07806-5000
1	ATTN: Harry Pebly
1	Department of the Army, Aerostructures Directorate, MS-266, U.S. Army Aviation R&T Activity - AVSCOM, Langley Research Center, Hampton, VA 23665-5225
1	NASA - Langley Research Center, Hampton, VA 23665-5225
1	U.S. Army Propulsion Directorate, NASA Lewis Research Center, 2100 Brookpark Road, Cleveland, OH 44135-3191
1	NASA - Lewis Research Center, 2100 Brookpark Road, Cleveland, OH 44135-3191
	Director, U.S. Army Materials Technology Laboratory, Watertown, MA 02172-0001
2	ATTN: SLCMT-TML
4	Authors

U.S. Army Materials Technology Laboratory  
Watertown, Massachusetts 02172-0001  
SURFACE ANALYSIS OF  $\text{Ln}_{2-x}\text{Ce}_x\text{CuO}_4$  ( $\text{Ln} = \text{Pr AND Nd}$ )  
SINGLE CRYSTALS GROWN BY THE TOP SEEDED  
SOLUTION METHOD.  
Louise C. Sengupta, Somnath Sengupta, Wendy E. Kosik,  
and J. Derek Demaree  
Technical Report MTL TR 92-34, May 1992, 14 pp-  
illus-tables.

AD UNCLASSIFIED  
UNLIMITED DISTRIBUTION  
U.S. Army Materials Technology Laboratory  
Watertown, Massachusetts 02172-0001  
SURFACE ANALYSIS OF  $\text{Ln}_{2-x}\text{Ce}_x\text{CuO}_4$  ( $\text{Ln} = \text{Pr AND Nd}$ )  
SINGLE CRYSTALS GROWN BY THE TOP SEEDED  
SOLUTION METHOD.  
Louise C. Sengupta, Somnath Sengupta, Wendy E. Kosik,  
and J. Derek Demaree  
Technical Report MTL TR 92-34, May 1992, 14 pp-  
illus-tables.

Large single crystals of  $\text{Ln}_{2-x}\text{Ce}_x\text{CuO}_4$  ( $\text{Ln} = \text{Pr AND Nd}$ ), the average size is approximately 5 mm x 5 mm x 1 mm, were grown by the Top Seeded Solution Growth (TSSG) technique. The optical constants of the crystals were determined by Variable Angle Spectroscopic Ellipsometry (VASE) and the results seem to indicate that a 1.5 eV absorption peak appears in the undoped material and is weakened and shifted downward in energy upon annealing. The compositions and crystal structure were examined using Rutherford Backscattering Spectroscopy (RBS) with ion beam channeling. Also, the effect of annealing on the crystalline structure was probed by ion beam channeling. The orientation and lattice parameters of the crystals were determined by X-ray diffraction and the superconductivity of the specimens was monitored using a SQUID magnetometer. The results indicate that the crystals grown by the TSSG method are very uniform in composition and well-oriented; however, analysis of the RBS data indicated up to 1% Pt inclusion in the crystals from contact with the Pt crucibles. The inclusion of Pt acted to quench the superconducting transition temperatures and Pt was found to substitute for Cu.

AD UNCLASSIFIED  
UNLIMITED DISTRIBUTION  
U.S. Army Materials Technology Laboratory  
Watertown, Massachusetts 02172-0001  
SURFACE ANALYSIS OF  $\text{Ln}_{2-x}\text{Ce}_x\text{CuO}_4$  ( $\text{Ln} = \text{Pr AND Nd}$ )  
SINGLE CRYSTALS GROWN BY THE TOP SEEDED  
SOLUTION METHOD.  
Louise C. Sengupta, Somnath Sengupta, Wendy E. Kosik,  
and J. Derek Demaree  
Technical Report MTL TR 92-34, May 1992, 14 pp-  
illus-tables.

Large single crystals of  $\text{Ln}_{2-x}\text{Ce}_x\text{CuO}_4$  ( $\text{Ln} = \text{Pr AND Nd}$ ), the average size is approximately 5 mm x 5 mm x 1 mm, were grown by the Top Seeded Solution Growth (TSSG) technique. The optical constants of the crystals were determined by Variable Angle Spectroscopic Ellipsometry (VASE) and the results seem to indicate that a 1.5 eV absorption peak appears in the undoped material and is weakened and shifted downward in energy upon annealing. The compositions and crystal structure were examined using Rutherford Backscattering Spectroscopy (RBS) with ion beam channeling. Also, the effect of annealing on the crystalline structure was probed by ion beam channeling. The orientation and lattice parameters of the crystals were determined by X-ray diffraction and the superconductivity of the specimens was monitored using a SQUID magnetometer. The results indicate that the crystals grown by the TSSG method are very uniform in composition and well-oriented; however, analysis of the RBS data indicated up to 1% Pt inclusion in the crystals from contact with the Pt crucibles. The inclusion of Pt acted to quench the superconducting transition temperatures and Pt was found to substitute for Cu.

AD UNCLASSIFIED  
UNLIMITED DISTRIBUTION  
U.S. Army Materials Technology Laboratory  
Watertown, Massachusetts 02172-0001  
SURFACE ANALYSIS OF  $\text{Ln}_{2-x}\text{Ce}_x\text{CuO}_4$  ( $\text{Ln} = \text{Pr AND Nd}$ )  
SINGLE CRYSTALS GROWN BY THE TOP SEEDED  
SOLUTION METHOD.  
Louise C. Sengupta, Somnath Sengupta, Wendy E. Kosik,  
and J. Derek Demaree  
Technical Report MTL TR 92-34, May 1992, 14 pp-  
illus-tables.

Large single crystals of  $\text{Ln}_{2-x}\text{Ce}_x\text{CuO}_4$  ( $\text{Ln} = \text{Pr AND Nd}$ ), the average size is approximately 5 mm x 5 mm x 1 mm, were grown by the Top Seeded Solution Growth (TSSG) technique. The optical constants of the crystals were determined by Variable Angle Spectroscopic Ellipsometry (VASE) and the results seem to indicate that a 1.5 eV absorption peak appears in the undoped material and is weakened and shifted downward in energy upon annealing. The compositions and crystal structure were examined using Rutherford Backscattering Spectroscopy (RBS) with ion beam channeling. Also, the effect of annealing on the crystalline structure was probed by ion beam channeling. The orientation and lattice parameters of the crystals were determined by X-ray diffraction and the superconductivity of the specimens was monitored using a SQUID magnetometer. The results indicate that the crystals grown by the TSSG method are very uniform in composition and well-oriented; however, analysis of the RBS data indicated up to 1% Pt inclusion in the crystals from contact with the Pt crucibles. The inclusion of Pt acted to quench the superconducting transition temperatures and Pt was found to substitute for Cu.